

Automatic identification of regions of interest with application to the quantification of DNA damage in cells.

Fred W M Stentiford^{*a}, Nick Morley^{**b}, Alison Curnow^{**b}
^aBTexact Technologies; ^bCornwall Dermatology Research Project

ABSTRACT

Visual systems that have evolved in nature appear to exercise a mechanism that places emphasis upon areas in a scene without necessarily recognising objects that lie in those areas. This paper describes the application of a new model of visual attention to the automatic assessment of the degree of DNA damage in cultured human lung fibroblasts. The visual attention estimator measures the dissimilarity between neighbourhoods in the image giving higher visual attention values to neighbouring pixel configurations that do not match identical positional arrangements in other randomly selected neighbourhoods in the image. A set of tools has been implemented that processes images and produces corresponding arrays of attention values. Additional functionality has been added that provides a measure of DNA damage to images of treated lung cells affected by ultraviolet light. The unpredictability of the image attracts visual attention with the result that greater damage is reflected by higher attention values. Results are presented that indicate that the ranking provided by the visual attention estimates compare favourably with an 'experts' visual assessment of the degree of damage. Potentially, visual attention estimates may provide an alternative method of calculating the efficacy of genotoxins or modulators of DNA damage in treated human cells.

Keywords: visual attention, saliency, segmentation, metadata, content, SCGE, comet assay, image analysis

1. INTRODUCTION

Visual systems that have evolved in nature appear to exercise a mechanism that places emphasis upon areas in a scene without necessarily recognising objects that lie in those areas. Organisms having the benefit of vision are thereby able to sense danger and direct attention rapidly towards the unusual without having to tolerate the initial delay of a recall from memory. Treisman and Gelade¹ in their feature-integration theory make the distinction between scenes that require relatively slow focussed attention to analyse and those which can be processed more rapidly during a preattentive stage. Evidence shows that it is relatively easy to spot a target "O" that pops out amongst a background of "N"s and "T"s, but time consuming to locate one's offspring in a school photograph. They posed, as others have done since, the question why features that distinguish a target from the background in preattentive vision when applied separately often do not when they appear in conjunction. Wolfe² emphasises that there is no clear distinction between slow serial and fast parallel mechanisms in visual search and that the evidence shows a continuum of search results in which both mechanisms perhaps play a part.

Desimone and Duncan³ in their review confirm that strengthening the perceived grouping between targets and background objects makes the background harder to ignore. Furthermore they suggest that there is little evidence that there are separate representations for different features such as orientation and colour in the cortex stating that cells that respond to a single type of stimulus have yet to be found. They conclude that preattentive vision is an emergent property of competitive interactions acting in parallel across the visual field and not the binding together of a set of separate feature measures.

Nothdurft⁴ has shown that the salience of targets in human vision is nearly always increased if multiple contrasts in orientation, luminance and motion are present. The addition was mostly nonlinear, which indicated that the underlying mechanisms were not independent and not separable as Desimone and Duncan suggest.

* fred.stentiford@bt.com; <http://www.btexact.com/>; BTexact Technologies, Adastral Park, Martlesham Heath, Ipswich, Suffolk, UK, IP5 3RE.

** nick.morley@cornwall-county.com; a.curnow@cornwall-county.com; Cornwall Dermatology Research Project, G14, PHLS, Royal Cornwall Hospitals Trust, Treliske, Cornwall, UK, TR1 3LQ.

Experiments by Reinagel and Zador⁵ using eye trackers show that subjects are attracted by image regions possessing high contrast and also by neighbourhoods in which pixel correlations drop off rapidly with distance. They observe that this strategy increases the entropy of the effective visual input and is in accord with measures of informativeness and cognitive surprise.

Early computational models⁶ of attention generate maps that encode the visual environment for different elementary features such as orientation of edges and colour contrast and combine these into an overall saliency map. The most conspicuous neighbourhoods are taken to be those that give rise to the most activity in the saliency map as a result of activity in corresponding feature maps. Many authors have put emphasis upon identifying specific features that are normally associated with saliency and combining these to produce such maps. Milanese *et al.*⁷ used five feature maps in their analysis of static scenes. After applying filters and passing the maps through a nonlinear relaxation process, they are averaged and thresholded to produce the saliency map. Itti *et al.*⁸ have defined a system which models visual search in primates. 42 features based upon linear filters and centre surround structures encoding intensity, orientation and colour, are used to construct a saliency map that reflects areas of high attention. Supervised learning is suggested as a strategy to bias the relative weights of the features in order to tune the system towards specific target detection tasks. They observed that salient objects appearing strongly in only a few dimensions may be masked by noise present in a larger number of dimensions.

Osberger and Maeder⁹ identified perceptually important regions by first segmenting images into homogeneous regions and then scoring each area using a number of intuitively selected measures. The approach was limited by the success of the segmentation techniques used. Luo and Singhal¹⁰ also devised a set of intuitive saliency features and weights and used them to segment images to depict regions of interest. The integration of the features was not attempted. Marichal *et al.*¹¹ used fuzzy logic to segment object boundaries before assigning levels of interest based upon a number of criteria. Zhao *et al.*¹² employed features reflecting size, distance from the centre of the image, boundary length, compactness and colour to determine region importance.

Walker *et al.*¹³ suggested that object features that best expose saliency are those which have a low probability of being mis-classified with any other feature. Mudge *et al.*¹⁴ also considered the saliency of a configuration of object components to be inversely related to the frequency that those components occur elsewhere. However, there is evidence that visual systems do not make use of sets of predefined features that we might intuitively believe to be important in attention mechanisms. Salient features are most likely to be different in different images and seem to emerge only at the time the images are processed. Furthermore, during preattentive vision rapid processing appears to take place in parallel in which visual neighbourhoods compete for attention. Reinagel *et al.* have shown that the neighbourhoods which are more likely to be distinctive and significant for preattentive vision are those that are quite small and only subtend a fraction of a degree to the eye.

In order to avoid an initial constraining commitment to predefined features the approach taken in this paper generates large numbers of random features as part of the process of measuring saliency. These features are tested on a trial and error basis and are selected for their capacity to distinguish small neighbourhoods from others in the image. The ease with which such features can be found serves as a plausible estimate of visual attention for each neighbourhood. This technique allows numerous nonlinear combinations of elementary measurements of colour and pixel relationships to compete and be assessed without suffering a combinatorial explosion. It would be expected that contrasts appearing in more than one dimension (eg both in luminance and edge orientation) would allow more scope for generating successful features and hence high visual attention scores.

The method has been successfully applied to the compression of static images¹⁵. By identifying regions of interest it is possible to achieve high compression rates without affecting the perceptual quality of certain categories of images. This paper describes an application of this model to the automatic assessment of the degree of DNA damage observed in cultured human lung fibroblasts¹⁶.

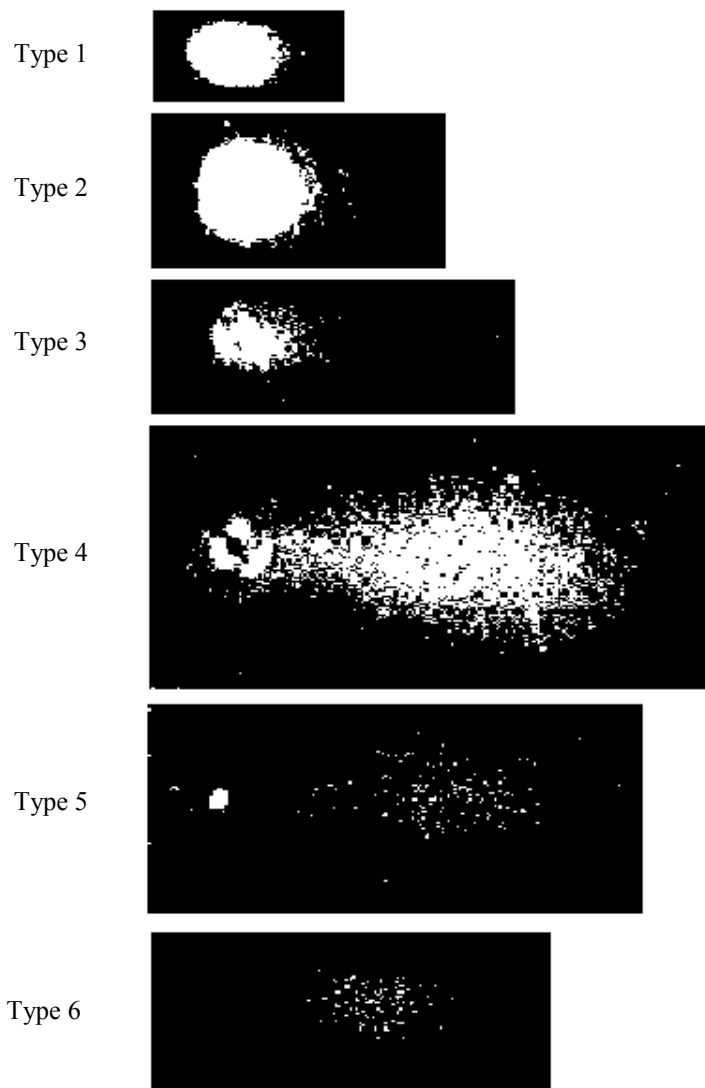


Fig. 1: Six-category visual scoring system devised from monochromatic digitalised images of actual comets, which represent the full range of DNA migration in incremental stages, with Type 1 representing little or no DNA migration through to Type 6, representing maximum DNA migration.

2. MEASURING DNA DAMAGE

In order to evaluate the genotoxicity of a substance, a method is required first to expose cellular DNA to the genotoxin, second to observe the DNA damage and third to quantify this damage.

In this study cultured human lung fibroblasts were embedded in a gel and, after transfer to glass microscope slides, irradiated with ultraviolet light for 90 seconds. The damage generated by this insult was then observed using the comet assay otherwise known as the single cell gel electrophoresis (SCGE), first introduced by Ostling and Johanson¹⁷ and modified by Singh *et al.*¹⁸. Briefly, the slides were placed in a high salt solution to lyse cellular and membrane proteins leaving cellular DNA free to migrate when electrophoresed. The slides were then transferred to an electrophoresis

buffer, left for forty minutes to allow time for the unwinding of double stranded DNA and for strand separation before they were electrophoresed at 20 V (~300 mA) for 24 minutes to cause DNA migration. Finally the slides were removed from the buffer, neutralised and left to air dry before the treated cells were stained with a fluorescent DNA marker (60 µg/ml ethidium bromide) so that they could be viewed using a light microscope with an epifluorescent attachment. During electrophoresis smaller fragments of DNA migrate further distances than larger fragments. The more lesions induced in cellular DNA the greater the number of smaller fragments produced and therefore the greater the amount of DNA which migrates away from the main DNA mass (nucleoid) – hence, the degree to which the DNA migrates after insult is a measure of damage the cell has sustained. Collins *et al.*¹⁹ devised a five-category visual scoring system to characterise ‘comets’ according to the degree of DNA migration (tail formation) and nucleoid (otherwise known as the head or body) shrinkage (the reduction in the head DNA mass). For this research reported here Collins’ scoring system was slightly modified to provide a six-category visual scoring system²⁰ (Fig. 1)

The level of DNA damage induced in the cells was evaluated using the visual scoring system. The visual scoring system is a rapid and reliable method of determining the differences between comets and therefore an effective system of evaluating genotoxins and modulators of DNA damage. However, while this method of scoring the comets rapidly produces qualitative data on the extent of DNA migration in single cells, it could be criticised for having a degree of subjectivity in assessing differences between comets. To counter this criticism the data is validated with robust non-parametric hypothesis tests for a significant difference. In contrast to the visual system, commercial computer imaging equipment and software is available for analysing the comets and producing continuous, quantitative data on different aspects of the comets such as the total area of a comet and the length to which the DNA has migrated. For example Comet assay II (Perceptive Instruments, Surrey, UK)²¹, can provide quantitative data on ten different comet parameters thus enabling parametric hypothesis testing and therefore a relatively sensitive method of analysing specific aspects of the comets. The parameters which correlate best with the visual scoring system are tail intensity, which is the percentage DNA in the tail, and tail moment (which combines the distance of DNA migration with relative amount)²². In order for tail intensity and tail moment to be calculated accurately a peak intensity in mean grey level has to be detected in the centre of the comet head as well as the detection of the entire migrated DNA, which possibly may be of very low intensity and therefore difficult to detect. In addition, image analysis by computer software can be adversely affected by artefact, comets overlaying each other and background fog, generated by fluctuations in the quality of the gel.

3. INFORMATION ATTENTION FRAMEWORK

The model of pre-attentive visual attention used in this paper relies upon the dissimilarity between neighbourhoods in the image. Visual attention values are higher when neighbouring pixel configurations do not match identical positional arrangements in other randomly selected neighbourhoods in the image. Neighbourhoods are matched if the colour values of pixels are separated by a distance less than a certain threshold in the chosen colour space²³.

Let a set of measurements \mathbf{a} correspond to a location \mathbf{x} in bounded n -space $(x_1, x_2, x_3, \dots, x_n)$ where

$$\mathbf{x} = (x_1, x_2, x_3, \dots, x_n) \text{ and } \mathbf{a} = (a_1, a_2, a_3, \dots, a_p)$$

Define a function \mathbf{F} such that $\mathbf{a} = \mathbf{F}(\mathbf{x})$ wherever \mathbf{a} exists. It is important to note that no assumptions are made about the nature of \mathbf{F} eg continuity. It is assumed that \mathbf{x} exists if \mathbf{a} exists.

Consider a neighbourhood N of \mathbf{x} where

$$\{\mathbf{x}' \in N \text{ iff } |x_i - x'_i| < \epsilon_i \forall i\}$$

Select a set of m random points S_x in N where

$$S_x = \{\mathbf{x}'_1, \mathbf{x}'_2, \mathbf{x}'_3, \dots, \mathbf{x}'_m\} \text{ and } \mathbf{F}(\mathbf{x}'_i) \text{ is defined.}$$

Select another location \mathbf{y} for which \mathbf{F} is defined.

Define the set $S_y = \{y'_1, y'_2, y'_3, \dots, y'_m\}$ where

$$\mathbf{x} - \mathbf{x}'_i = \mathbf{y} - \mathbf{y}'_i \text{ and } \mathbf{F}(\mathbf{y}'_i) \text{ exists.}$$

The neighbourhood of \mathbf{x} is said to match that of \mathbf{y} if

$$|F_j(\mathbf{x}) - F_j(\mathbf{y})| < \delta_j \text{ and } |F_j(\mathbf{x}'_i) - F_j(\mathbf{y}'_i)| < \delta_j \quad \forall i,j.$$

In general δ_j is not a constant and will be dependent upon the measurements under comparison ie.

$$\delta_j = f_j(\mathbf{F}(\mathbf{x}), \mathbf{F}(\mathbf{y}))$$

A location \mathbf{x} will be worthy of attention if a sequence of t neighbourhoods matches only a small number of other neighbourhoods in the space.

In the case of a two-dimensional still image, m pixels \mathbf{x}' are selected in the neighbourhood of a pixel \mathbf{x} (Fig. 2). Each of the pixels might possess three colour intensities, so $\mathbf{F}(\mathbf{x}') = \mathbf{a} = (r, g, b)$.

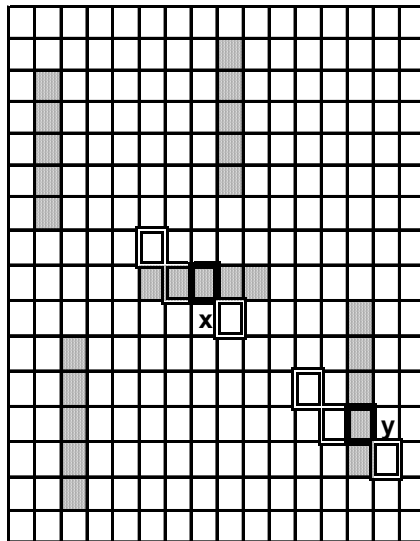


Fig. 2: Neighbourhood at \mathbf{x} mismatching at \mathbf{y} .

The neighbourhood of a second pixel \mathbf{y} matches the first if the colour intensities of all $m + 1$ corresponding pixels have values within δ of each other. Pixels \mathbf{x} that achieve high mismatching scores over a range of t neighbouring pixel sets S_x and pixels \mathbf{y} are assigned a high estimate of visual attention. This means that pixels possessing novel colour values that do not occur elsewhere in the image will be assigned high visual attention estimates. It also means that neighbourhoods that span different coloured regions (eg edges) are naturally given high scores if those colour adjacencies with those orientations only occur rarely in the scene.

The gain of the scoring mechanism is increased significantly by retaining the pixel configuration S_x if a mismatch is detected, and re-using S_x for comparison with the next of the t neighbourhoods. If however, S_x subsequently matches another neighbourhood, the score is not incremented, and an entirely new configuration S_x is generated ready for the next comparison. In this way competing configurations are selected against if they contain little novelty and turn out to represent structure that is common throughout the image. Indeed it is likely that if a mismatching pixel configuration is generated, it will mismatch again elsewhere in the image, and this feature in the form of S_x once found, will accelerate the rise of the visual attention score provided that the sequence is not subsequently interrupted by a match.

The size of neighbourhoods is specified by the maximum distance components ϵ_i to the pixel being scored. The neighbourhood is compared with the neighbourhoods of t other randomly selected pixels in the image that are more

than a distance epsilon from the boundary. Typically $\epsilon_i = 4$ and $t = 100$, with $m = 3$ neighbouring pixels selected for comparison. Larger values of m and the ϵ_i are selected according to the scale of the patterns being analysed. Increasing the value of t improves the level of confidence of the detail in the attention estimate display.

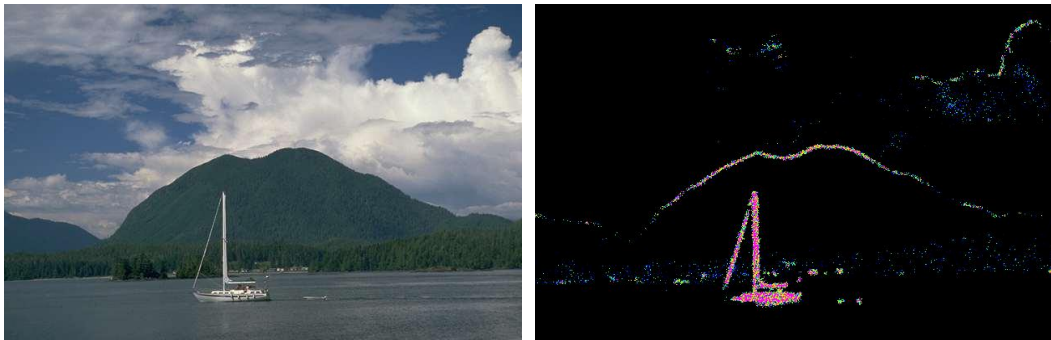


Fig. 3: Image and visual attention map

The visual attention estimator has been implemented as a set of tools that processes images and produces corresponding arrays of attention values. The attention values are thresholded and those above the threshold are displayed using a continuous spectrum of false colours with the maximum scores being marked with a distinctive colour. The analysis has yielded a number of promising results on real images (Fig. 3). Additional functionality has been added that provides a new measure of DNA damage to images of treated lung cells affected by ultraviolet light. The unpredictability of the image attracts visual attention with the result that greater damage is reflected by higher attention values.

4. RESULTS

29 unlabelled grey level images of cells suffering various levels of damage were supplied for analysis. It was immediately apparent that the distribution of grey levels within each image was very broad with no special features being immediately apparent. This meant that as the visual attention measure associated high scores with neighbourhoods possessing unique configurations of grey levels, it simply highlighted the whole comet area and did not identify any special features in individual comet images. This would not have been the case had a large number of comets been present in a composite image in which comets were likely to share similarities of appearance, and hence reduce the likelihood of unique structures being present.

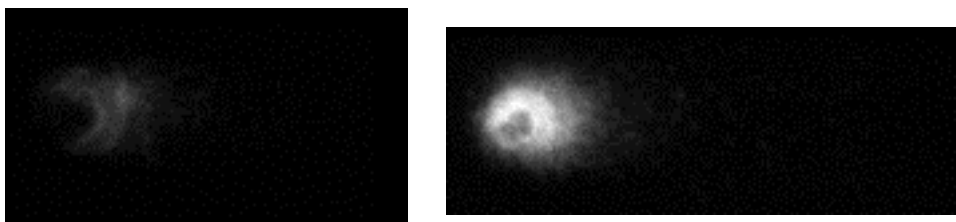


Fig. 4: Comet images (ID = 2, 15)

However, it was also apparent that the grey level distributions were significantly different in many of the images (Fig. 4). This was due mainly to the nature of the material in the comets and differences in the level of damage induced in the cells. Furthermore illumination can be affected by a gradual deterioration in the DNA marker. Unfortunately the visual attention measure has no way of distinguishing pre-processing artefacts from anomalies actually present in the content and tended to highlight irrelevant features eg relatively rare bright areas. This problem could again be mitigated by processing larger numbers of comets so that experimental variability is factored out. Alternatively each comet image could be normalised in an appropriate fashion; this was not attempted because of the inevitable danger of introducing intuitive judgements into the processing that would not be generically applicable to other data. However, several normalisation strategies do merit further study in this application.

In view of these problems it was decided to crop each comet image and prepare a single 911 x 576 pixel image that depicted all 29 comets. This would allow the visual attention mechanism to highlight anomalies within the context of the total data set. It was also decided that thresholding the composite image would remove most of the distracting grey level variability between comets and at the same time preserve the DNA migration in the resulting image (Fig. 5). Care was taken to ensure that each comet image was separated from others by a pixel distance greater than $2\epsilon_i$ (ie ≥ 9) to prevent attention scores being raised because of arbitrary adjacencies arising from the layout.

The composite image was processed on a 866MHz Pentium in 183 seconds with parameters $\{t=100; m=3; \epsilon_i=3\}$ to produce an array of attention scores. The scores are represented in a map (Fig. 6) generated using pixels scoring more than 80% of the overall maximum score and false colours assigned to represent scores in this range. Pixels with the highest attention scores were tagged and displayed with a distinctive colour in the map. The number of maximum scoring pixels associated with each comet area was used as the measure of cell damage (Table 1).

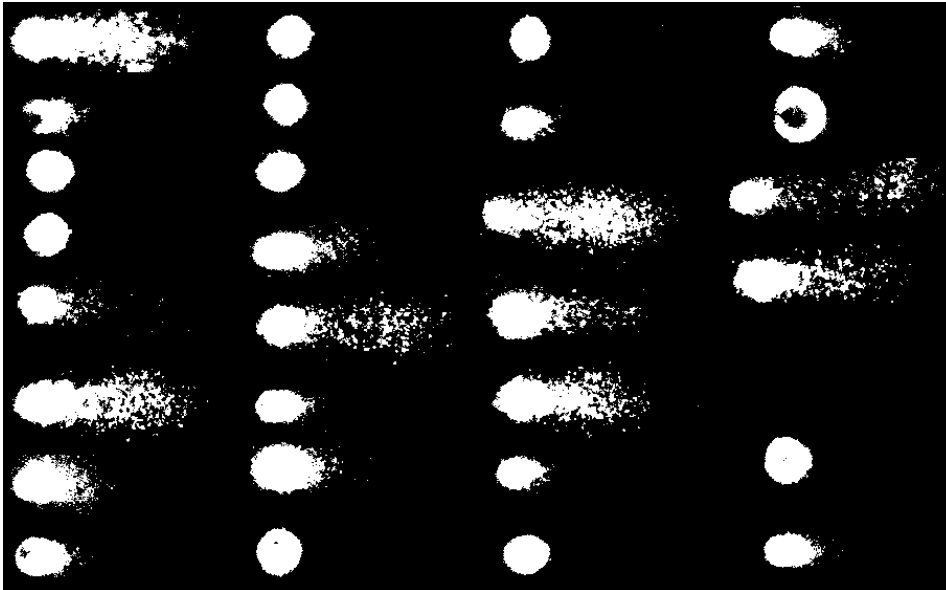


Fig. 5: Thresholded comet images (IDs = 1 - 29 top to bottom left to right)

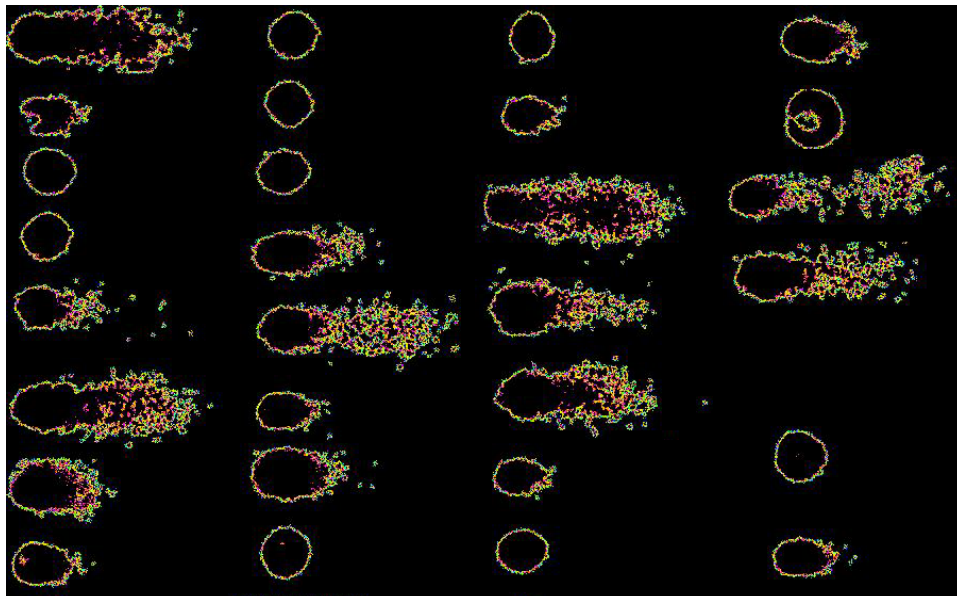


Fig. 6: Visual attention map

Comet ID	Mean Comet Score	Attention Score	Area (pixels)	Score:Area Ratio	Tail Length
26	4	512	2138	0.24	14.63
13	4	628	3071	0.20	9.16
19	4	724	5118	0.14	18.40
27	4	394	3115	0.13	11.23
5	4	195	1567	0.12	11.53
20	4	358	2938	0.12	9.75
21	4	453	3804	0.12	11.90
7	3	297	2510	0.12	6.28
6	4	545	4813	0.11	12.86
12	3	225	2196	0.10	5.62
2	3	116	1162	0.10	2.81
1	4	393	5569	0.07	10.71
18	3	80	1149	0.07	4.95
22	3	78	1124	0.07	3.77
15	3	176	2574	0.07	7.83
29	3	88	1342	0.07	5.10
24	3	115	1777	0.06	5.25
8	3	96	1520	0.06	9.31
14	3	76	1297	0.06	3.62
25	2	101	1789	0.06	1.33
23	2	54	1298	0.04	2.29
16	2	61	1497	0.04	1.40
3	2	57	1431	0.04	1.40
11	2	54	1360	0.04	2.14
10	2	49	1242	0.04	2.66
28	2	58	1582	0.04	1.11
3	2	45	1361	0.03	1.55
9	2	43	1355	0.03	2.96
17	2	36	1267	0.03	2.44

Table 1: Attention scores in decreasing score/area ratio

Each cell had been assigned a Mean Comet Score (MCS) which reflected a visual measure of damage: 2 - little damage; 3 - medium damage; 4 - significant damage (Fig. 1). The area of each displayed comet in pixels and the length of the comet tail were also recorded. The results in table 1 are ordered in decreasing values of the ratio of attention score to comet area. Most comets were ordered correctly in relation to the MCS, however, two comets (IDs = 1,7) are out of position although still lie quite close to the correct subjective assessment.

Amongst many other possible measures, comet tail length produces one of the best orderings in this set of images, but two comets are again out of position (IDs = 2,14). Comet image no. 1 is clearly badly damaged, but the image capture and thresholding has left the tail much less fragmented than the others and hence produces lower scores in proportion to its area. Careful inspection of comet no. 7 reveals that although the damage does not appear to spread over a great area, the disruption is more finely divided than other comets in the experiment and perhaps merits closer inspection to determine the reasons for this.

5. CONCLUSIONS

The results of this study of cells exposed to a genotoxin show that the DNA damage estimated by attention values are comparable to the estimates produced by a skilled analyst using a reliable visual scoring system. Furthermore, the visual scoring system only produces qualitative data that is validated with non-parametric statistical tests, and it is possible that measures of visual attention will offer quantitative data on the overall nature of the comet and enable the detection of more subtle effects. However, the attention measures cannot discriminate between artefacts and comets, and comets overlaying each other. Some manual involvement is therefore necessary to exclude extraneous material.

Current automated image analysis software presently exists that offers an alternative method of evaluating DNA damage to treated cells. These methods detect a number of different comet parameters and provide quantitative data that allows parametric hypothesis statistical analysis derived from specific features of the comet like tail intensity and other aspects known to be relevant. In future attention values may provide an alternative automated image analysis system which provides quantitative data based on the entire comet and not limited to a set of predetermined feature measurements.

REFERENCES

1. A. M. Treisman and G. Gelade, "A feature-integration theory of attention", *Cognitive Psychology*, **12**, pp. 97-136, 1980.
2. J. M. Wolfe, "Visual Search" in "Attention" edited by H Pashler, Psychology Press, 1998.
3. R. Desimone and J. Duncan, "Neural mechanisms of selective visual attention", *Annu. Rev. Neurosci.*, **18**, pp. 193-222, 1995.
4. H. C. Nothdurft, "Saliency from feature contrast: additivity across dimensions", *Vision Research*, **40**, pp. 1183-1201, 2000.
5. P. Reinagel and M. Zador, "Natural scene statistics at the centre of gaze", *Network: Comp. Neural Syst.*, **10**, pp. 341-350, 1999.
6. C. Koch and S. Ullman, "Shifts in selective visual attention: towards the underlying neural circuitry", *Human Neurobiol.*, **4**, pp. 219-227, 1985.
7. R. Milanese, S. Gil and T. Pun, "Attentive mechanisms for dynamic and static scene analysis", *Optical Engineering*, **34**, No 8, pp. 2420-2434, August 1995.
8. L. Itti, C. Koch and E. Niebur, "A model of saliency-based visual attention for rapid scene analysis", *IEEE Trans PAMI*, **20**, No 11, pp. 1254-1259, November 1998.
9. W. Osberger and A. J. Maeder, "Automatic identification of perceptually important regions in an image", 14th IEEE Int. Conference on Pattern Recognition, 16-20th August 1998.
10. J. Luo and A. Singhal, "On measuring low-level saliency in photographic images", *IEEE Conf. On Computer Vision and Pattern Recognition*, June 2000.
11. X. Marichal, T. Delmot, C. De Vleeschouwer, V. Warscotte and B. Macq, "Automatic detection of interest areas of an image or of a sequence of images", *IEEE Int. Conf on Image processing*, 1996.
12. J. Zhao, Y. Shimazu, K. Ohta, R. Hayasaka, and Y. Matsushita, "An outstandingness oriented image segmentation and its application", *Int. Symposium on Signal Processing and its Applications*, August 1996.
13. K. N. Walker, T. F. Cootes and C. J. Taylor, "Locating Salient Object Features", *British Machine Vision Conference*, 1998.
14. T. N. Mudge, J. L. Turney and R. A. Volz, "Automatic generation of salient features for the recognition of partially occluded parts", *Robotica*, **5**, pp. 117-127, 1987.
15. F. W. M. Stentiford, "An estimator for visual attention through competitive novelty with application to image compression", 22nd Picture Coding Symposium, Seoul, April 2001.

16. A. Curnow, N. Salter, N. Morley and D. Gould, "A preliminary investigation of the effects of arsenate on irradiation-induced DNA damage in cultured human lung fibroblasts", *Journal Toxicology and Environmental Health, Part A*, **63**: pp. 101-112, 2001.
17. O. Ostling and K. J. Johanson, "Microelectrophoretic study of radiation-induced DNA damages in individual mammalian cells", *Biochemistry Biophysics Research Communication*, **123**, pp. 291-8, 1984.
18. N. P. Singh, M. T. McCoy, R. R. Tice and E. L. Schnieder, "A simple technique for quantitation of low levels of DNA damage in individual cells", *Experimental Cell Research*, **175**, pp. 184-191, 1988.
19. A. R. Collins, M. Ai-guo and S. J. Duthie, "The kinetics of repair of oxidative DNA damage (strand breaks and oxidized pyrimidines) in human cells", *Mutation Research*, **336**, pp. 69-77, 1995.
20. J. F. Kendall, "Single cell gel electrophoresis-based investigations of UVR- and visible-induced single strand breakage in cultured human cells", Doctor of Philosophy Thesis, University of Plymouth, pp. 78, 1999.
21. <http://www.perceptive.co.uk/>
22. P. J. McCarthy, S. F. S. Sweetman, P. G. McKenna and McKelvey-Martin, "Evaluation of manual and image analysis quantification of DNA damage in the alkaline comet assay", *Mutagenesis*, **12**, pp. 209-214, 1997.
23. G. Sharma and H. J. Trussell, "Digital Color Imaging", *IEEE Trans on Image Processing*, **6**, No 7, July 1997, pp. 901-932.